Formation of ceramic microstructures: honeycomb patterned polymer films as structure-directing agent†

Lei Li,*[a] Jian Li,[a] Yawen Zhong,[a] Caikang Chen,[a] Yi Ben,[b] Jianliang Gong[a] and Zhi Ma*[c]

Received 13th February 2010, Accepted 30th March 2010
First published as an Advance Article on the web 26th May 2010
DOI: 10.1039/c0jm00405g

Here, we show a facile and versatile method preparing highly ordered ceramic microstructures on solid substrates by pyrolyzing UV cross-linked copolymer films to circumvent the expensive lithographic technique. The employed block copolymer, poly(dimethylsiloxane)-*block*-polystyrene (PDMS-*b*-PS), in this study was synthesized by controlling radical polymerization. The highly ordered microporous polymer films were formed using a static breath figure process. After 4 h UV irradiation, the PS composition was effectively cross-linked. The cross-linked microporous polymer matrix served as a structure-directing agent in the following pyrolysis process, in which the PDMS composition was converted into silica to form honeycomb structured micropatterns on the substrate. The chemical components of the ceramic microstructures were adjusted by simply mixing different functional precursors. Moreover, the ceramic microstructures on substrate could be replicated to prepare textured PDMS stamps. This simple technique offers new prospects in the fields of micropatterns, soft lithography and templates.

Introduction

Obtaining micro- and nano-scale patterns with easy to use and cheap techniques has been the center of interest in many different fields in the past decades.[1] Microstructured ceramic materials are of interest in miniaturized systems because of not only their high thermal and chemical resistance but also their hardness and possible functional properties, such as high dielectric constants, photonic crystals, ionic conductivity and catalytic activity.[2] In microelectromechanical systems (MEMS), most of the ceramic materials used are in the form of thin films. It is clearly inefficient to scratch microstructures into such thin ceramic films. Recent innovations in the area of micro- and nanofabrication have created unique opportunities for patterning surfaces with features and lateral dimensions. The widespread efforts to utilize a variety of hard templating techniques include molding, direct writing, photolithography, colloidal crystal self-assembly and substrate-surface modification.[3] However, the dimensions of the skeletal structures are fixed and dependent upon the size of the templates, and the cost raises the whole process price.

Because of the drive toward cheaper and faster processes, a greater importance has been given to phenomena such as self-assembly and other self-organization processes.[4] The breath figure (BF) process is one of the most promising self-assembling strategies for the fabrication of large size patterns having an ordered two-dimensional array of holes.[5] The principle of this method is described as follows. Rapid evaporation of solvent causes the temperature of the solution surface to drop initiating the nucleation of water droplets. Influenced by the surface convection and capillary attractive force, the condensed water droplets self-organize into a hexagonal array before their coagulation with each other. During this process, the polymer dissolved in the solution is absorbed to the interface between the water and the polymer solution, which stabilizes the water droplets and prevents their coagulation. With continuing solvent evaporation, the polymer solidifies and molds around the water droplets, acting as sacrificial template. Periodic water droplets are packed and return to ambient temperature, thus allowing the condensed water micro-droplets to subsequently evaporate, and leaving behind the observed microporous structures. Various types of polymers can be fabricated as a honeycomb-patterned film with controlled pore size, ranging from hundreds of nanometres to hundreds of microns.[6] The simple method offers new prospects in the field of microporous films, as well as other technical advantages of low-cost and large area applicability.[7] An organometallic conjugated polymer precursor was shaped into an hexagonal array and then pyrolyzed to microstructured Si–C–Co and Si–O–Co ceramics.[6a] Also, a sol–gel process induced by soaking a microporous polymer film bearing anhydride groups into 3-aminopropyltrimethoxysilane (APTES) created a porous silica film.[8] The applicability of the mentioned methods is limited by the time-consuming synthesis and particular chemical reactions. A much simpler and versatile preparation of ceramic microstructures is more desirable.

In this article, we report a facile methodology to prepare highly ordered ceramic micropatterns on solid substrates by pyrolyzing UV cross-linked polymer microporous films. The

[a]*College of Materials, Xiamen University, Xiamen, 361005, P. R. China. E-mail: lilei@xmu.edu.cn; Fax: +86-592-2183937; Tel: +86-592-2186296*
[b]*Analysis & Test Center, Xiamen University, Xiamen, 361005, P. R. China*
[c]*Shanghai Institute of Organic Chemistry, Chinese Academy of Sciences, Shanghai, 200032, P. R. China. E-mail: mazhi728@sioc.ac.cn*

† Electronic supplementary information (ESI) available: Fig. S1: Photograph of sunlight diffraction obtained from a honeycomb structured PDMS-*b*-PS film on glass substrate after 4 h UV irradiation. Fig. S2: XPS core level scans of Si and O after pyrolysis of honeycomb structured PDMS-*b*-PS film. Fig. S3: Photograph of sunlight diffraction obtained from a honeycomb structured silica on glass substrate. See DOI: 10.1039/c0jm00405g

versatility of this fabrication process is demonstrated by preparing ordered ceramic micropatterns with different chemical species on solid substrates, simply through mixing different functional precursors. Moreover, the patterns can be replicated by siloxane-based soft stamps, which have widespread use in soft lithography. To circumvent the expensive lithographic technique, the reported methodology apparently provides a facile preparation of patterned ceramic microstructures that may be useful for engineering applications.

Experimental

Materials

Tetrabutyl titanate ($Ti(OC_4H_9)_4$) was obtained from Sinopharm Chemical Reagent Co. Ltd. Cobalt(III) acetylacetonate ($Co(acac)_3$) and ferrocene were purchased from Alfa Aesar. Monohydroxy terminated polydimethylsiloxane (PDMS-OH) (Aldrich, M_n = 4670 g mol^{-1}) and 2-bromo-2-methylproponyl bromide (Acros, 98%) were used as received without further purification. Triethylamine was supplied by Sinopharm Chemical Reagent Co. Ltd. and stirred over CaH_2 for 4 h at room temperature, then distilled and stored over 4-Å molecular sieves. Tetrahydrofuran (THF) was refluxed over sodium/benzophenone and distilled under nitrogen before use. Copper(I) bromide (Cu^IBr) (Acros, 99.9%) was stirred in glacial acetic acid overnight and filtered though a Buchner funnel then washed three times with ethanol and diethyl ether, dried in vacuum overnight, and stored under nitrogen. 4,4′-Di(5-nonyl)-2,2′-bipyridine (dNbpy) was obtained from Aldrich Chemical Co. and used as received. Styrene (Aldrich, 99%) was stirred over calcium hydride under nitrogen and distilled before use. All other chemicals obtained were used as received.

Synthesis of PDMS-Br macroinitiator

An oven-dried 100 mL Schlenk flask with a magnetic stir bar was charged with anhydrous THF (60 mL), PDMS-OH (1.5 mL, 0.31 mmol), triethylamine (0.17 mL, 1.24 mmol) and 2-bromo-2-methylpropionyl bromide (0.077 mL, 0.62 mmol) and left for 36 h at ambient temperature. After filtration of the hydrochloride salt, the solution was placed under vacuum to remove solvent. The resulting oil was taken up in dichloromethane (40 mL) followed by washing with saturated sodium hydrogen carbonate solution (50 mL). The resulting organic layer was isolated, dried over magnesium sulfate, and filtered. Then the oil-like product was obtained after removing the volatiles at ambient temperature under vacuum.

Synthesis of PDMS-*b*-PS diblock copolymer

PDMS-Br macroinitiator (1 mL, 0.21 mmol), styrene (2.41 mL, 21 mmol), Cu^IBr (60.25 mg, 0.42 mmol), dNbpy (131 mg, 0.84 mmol) were added to a Schlenk flask sealed with rubber. The flask was then degassed by five cycles of freeze–pump–thaw. During the final cycle, the flask was back-filled with nitrogen and then immersed in an oil-bath thermostated at 110 °C. After the polymerization for 24 h, the mixture was diluted in 50 mL of THF and then filtered through neutral alumina to remove the copper salt. Then the mixture was added dropwise to 600 mL of methanol. The resulting precipitate was obtained by filtration and dried over night at 60 °C under vacuum. The relative molecular weight and molecular weight distribution of the block copolymer were 26 000 and 1.22, respectively, as determined by gel permeation chromatography (GPC).

Preparation of microporous PDMS-*b*-PS films

The glass substrates (0.5 × 1 cm^2) were cleaned by detergent and acetone successively and air dried. A static breath-figure process was operated in a 25 mL straight-mouth glass bottle with a cap. Saturated relative humidity in the vessel was achieved beforehand by adding 2 mL distilled water into the bottle. A piece of cleaned glass substrate was adhered on the top of a plastic stand with double sided tape and placed into the glass vessel. The glass substrate was 1 cm above the liquid level. Polymer solutions with different concentrations were prepared by dissolving PDMS-*b*-PS in carbon disulfide (CS_2). The micropatterned film was prepared by casting 100 μL of the polymer solution onto the substrate with a microsyringe. With organic solvent volatilization, the transparent solution surface became turbid. The film was then taken out for microscope observation after complete solvent evaporation.

Preparation of microporous polymer/functional precursor hybrid films

Block copolymer PDMS-*b*-PS and functional precursor were mixed with a fixed weight ratio (3/1, w/w) and dissolved in CS_2. The solution concentration was 40 mg mL^{-1}. The honeycomb film was prepared by casting 100 μL of solution onto the substrate with a static BF process as mentioned above.

Photochemical cross-linking and pyrolyzing process

The photochemical cross-linking was performed at 30 °C in a UVO cleaner ZWLH-5 (Tianjin, China) in the presence of air, by exposing the polymer thin films into UV light. The cleaner generated UV emissions at a wavelength of 254 nm and power of 500 W. The distance between the UV source and the film surface was 10 cm. After 4 h UV exposure, the cross-linked films were heated to 450 °C within 2 h and held for another 5 h under air atmosphere.

Characterization and apparatus

Relative molecular weights and molecular weight distributions were determined by GPC using a Waters GPC 1515 with THF as the eluent and polystyrene standards as the references. Scanning electronic microscopy (SEM) images were obtained using a Hitachi S4800 scanning electron microscope. A 10 keV electron beam was used for the observation with a working distance of 10 mm in order to obtain secondary electron images. Atomic force microscopy (AFM) measurements were carried out in the tapping mode with a Seiko Instruments SPA400. X-Ray photoelectron spectroscopy (XPS) spectra were acquired with a PHI Quantum 2000 spectrometer using monochromated X-rays from an Al-Kα source with a take-off angle of 45° from the surface plane. Grazing-incidence X-ray diffraction (GIXRD) measurements were collected with a PANalytical X-ray diffractometer

using the Cu-Kα line (1.54 Å) from an X-ray generator operated at 40 kV and 40 mA.

Results and discussion

Formation of silica microstructures on substrates

The fabrication process of robust ceramic micropatterns on a substrate is schematically shown in Fig. 1. First, PDMS-*b*-PS diblock copolymer was dissolved in CS_2. After the solution was cast on the substrate by a microsyringe, rapid evaporation of solvent caused the temperature of the solution surface to drop and initiated the nucleation of water droplets (Fig. 1a). After evaporation of solvent in saturated relative humidity, a highly regular microstructured polymer film was formed (Fig. 1b). In the following UV irradiation, not only the PS composition was effectively cross-linked with improved thermal stability but also the honeycomb structures were well preserved (Fig. 1c). The cross-linked polymer matrix acted as a structure-directing agent in the subsequent pyrolysis process, where the PDMS composition was converted into the skeleton of the micropatterns. Eventually, ceramic micropatterns were formed on the substrate after completely decomposing the PS component (Fig. 1d).

Although a variety of polymers have been used to prepare honeycomb structured films by the BF method, the pattern forming mechanism is not yet well understood. Different polymers require different preparation conditions, which makes the process more empirical. Breath-figure templating requires that the solute prevents water droplets from undergoing coalescence. This requirement is met by a wide range of colloidal materials, including star-shaped polymers and block copolymers because of their high segment density.[6] Additionally, a highly volatile, water-immiscible organic solvent, such as CS_2 or chlorinated solvents, is believed to be another prerequisite for the successful formation of honeycomb structured porous films.[6d,9] The rapid solvent evaporation leads to a decrease in solution temperature and facilitates the condensation of water droplets on the solution surface. In a typical dynamic process, an airflow is applied to control the evaporation rate of solvent and the humidity. The rate of evaporation varies during the evolution of the casting process. The nonisothermal and nonequilibrium nature of the process often leads to poor repeatability of the microporous structures. Here, a much simpler static method as mentioned in the Experimental section is employed to fabricate micropatterned films to avoid uncertainties and facilitate batch processes.

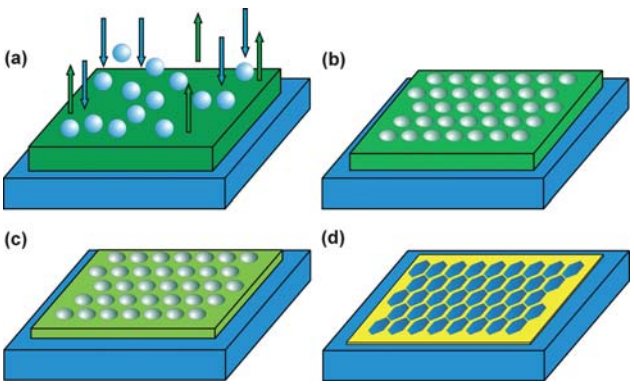

Fig. 1 Schematic illustration of fabrication of ceramic micropatterns on substrates. (a) Evaporation of solvent causes the temperature of the solution surface to drop and initiates the nucleation of water droplets. (b) A highly regular microstructured polymer film is formed on the substrate after total evaporation of solvent under high humidity. (c) The polymer matrix is cross-linked and the honeycomb structures are preserved after the photochemical process. (d) Robust ceramic micropatterns on the substrate are formed after pyrolysis.

The morphologies of the formed microporous structures during the static BF process are mainly controlled by the solution concentrations. No regular patterns are formed on the film surface when the solution concentration is less than 10 mg mL^{-1} (Fig. 2a). With increasing the concentration to 40 mg mL^{-1}, the obtained film on the substrate exhibits an interesting nacre color (Fig. 2b), which is ascribed to the sunlight diffraction decomposed by highly ordered structures and interference effects.[10] A more precise microscopy study by AFM and SEM is shown in Fig. 2c and d, respectively.

The top surface of the film displays open pores with average diameter of 1430 nm and standard deviation of 74 nm. Peeling off the top layer of the film using adhesive tape (Scotch Tape, 3M), highly ordered honeycomb structures with thin walls are observed. The underneath honeycomb structures show a uniform pore diameter of 3150 nm with a standard deviation of 72 nm. Their wall thickness is 140 ± 31 nm. Either top or cross-sectional view (Fig. 2e) reveals that the resultant film has a monolayer of independent pores on a dense polymer stratum without network structures. Single layer microporous structures are crucial for the formation of regular ceramic patterns on substrates as discussed below. Upon further increasing the solution concentration to 70 mg mL^{-1}, multiple layers of pores are formed, as shown in Fig. 2f.

Polymer precipitation is believed to be a key element in producing a regular hole pattern.[5c] When the solution concentration is comparably low, the solution viscosity is too low to encapsulate the droplets or prevent their coalescence, resulting in the formation of disordered structures. With the increasing of solution concentration (solution viscosity), water droplets can be effectively trapped onto the solution surface so that highly ordered patterns appear. The formation of ordered patterns contributes to the convection generated in the evaporating solution and the lateral capillary force between the adjacent droplets (Marangoni effect). The evaporation rate of solvent in a more concentrated solution is reduced so that the temperature difference (ΔT) between the atmosphere and the solution surface decreases. As the growth rate (R) of droplets is governed by the relation $dR/dt \sim \Delta T^{0.8}$,[11] a lower growth rate of droplets is obtained due to the reduced temperature difference. In addition, the increased viscosity will weaken the convection in the solution, which is not beneficial to the ordered packing of droplets, so that the pore size is slightly reduced and the packing of pores becomes disordered. Moreover, the condensed water droplets do not coalesce, but start to sink into the solution, propagate through the film and form multiple layers of pores.

The obtained honeycomb structures began to melt and collapse upon heating up to 100 °C (the glass transition temperature, T_g, of PS and PDMS are 100 and −120 °C, respectively), and totally disappeared at 130 °C. No special features were found on the substrate after pyrolysis. The poor

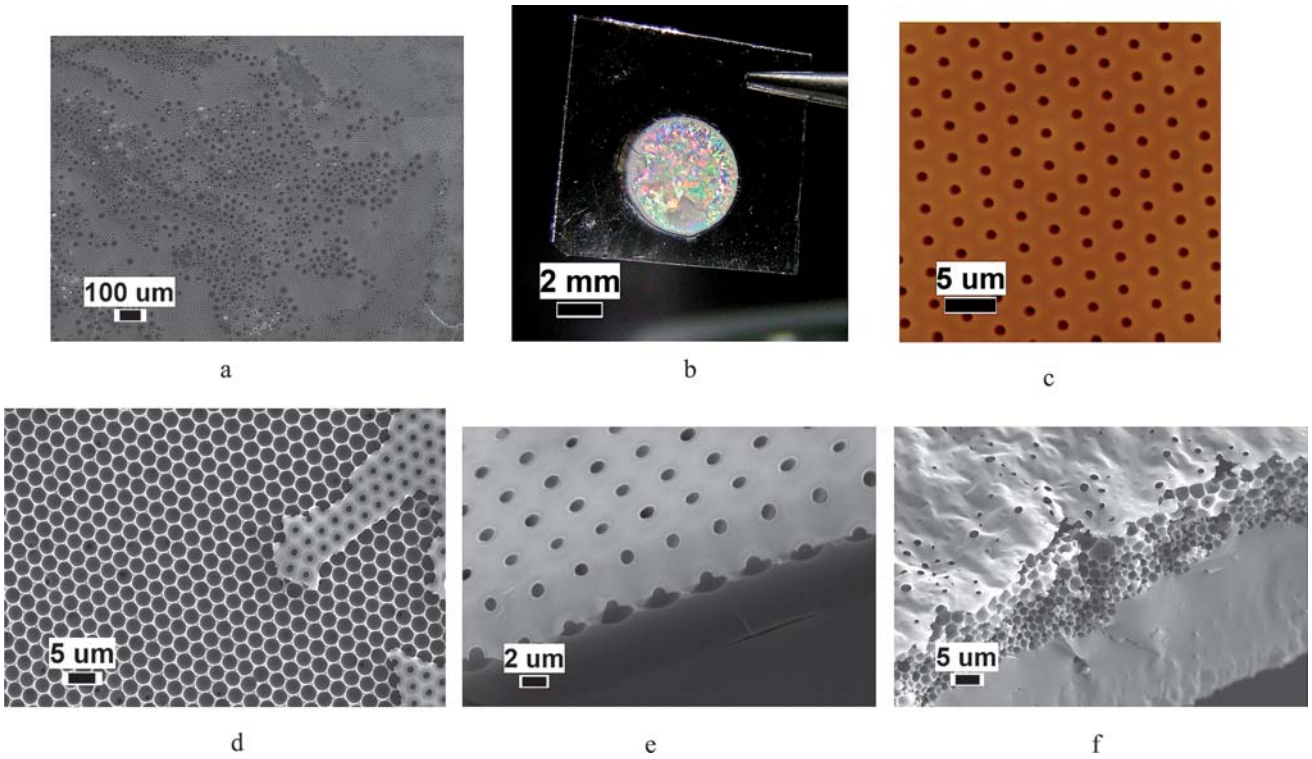

Fig. 2 (a) Scanning electron micrographs of micropatterns on the polymer film surfaces. The films are prepared by casting from PDMS-*b*-PS/CS_2 solution with a concentration of 10 mg mL^{-1}. (b) Photograph of sunlight diffraction obtained from a honeycomb structured PDMS-*b*-PS film on glass substrate casting from a solution of 40 mg mL^{-1}. (c) Topographic and (d) SEM images of the honeycomb structured PDMS-*b*-PS film. (e) Cross-section view of the honeycomb structured PDMS-*b*-PS film. (f) SEM image of PDMS-*b*-PS film casting from a solution of 70 mg mL^{-1}.

thermal stability makes the structure-directing action of the polymer matrix invalid. Cross-linkage should be an efficient method targeting the stable film structure against solvents and heat annealing.[12] Recently, we reported that a UV cross-linked polymer matrix with improved thermal stability served as a structure-directing agent to fabricate regular inorganic micropatterns.[13] Here, a similar photochemical cross-linking process by deep UV irradiation was employed to cross-link the PS matrix and improve its thermal stability. The photochemically cross-linking mechanism of PS has been elucidated thoroughly and is briefly described as follows.[14] Radicals are formed during the UV irradiation by abstracting hydrogen atoms from polymer molecules. Although the movement of macromolecules in the solid state is restricted, free radicals can migrate along the polymer chain until they are trapped by other free radicals or impurities. When two radicals are near to each other cross-linking may occur (Scheme 1).

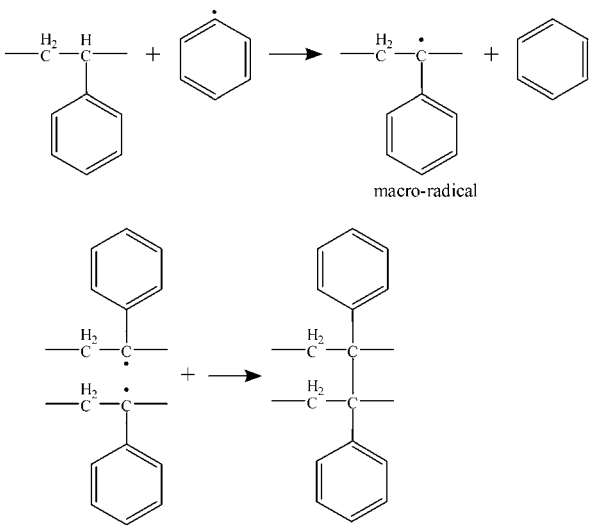

Scheme 1

Compared with chemical cross-linking, the photochemical cross-linking process is operated at room temperature and easier to control, which is helpful for the preservation of ordered structures after UV treatment.[12d,12e,13] After 4 h UV irradiation, the beautiful rainbow color did not disappear (see ESI†, Fig. S1), indicative of well preserved microporous structures. Close microscope examinations are shown in Fig. 3a (top-view) and 3b (cross-section view), respectively. The honeycomb patterns and spatial structures in the microporous film are highly maintained without collapse. Compared with the as-prepared films, the walls of pores in the cross-linked films become slightly thinner because of partial photo-degradation of PS during the UV irradiation. However, no film thickness change is observable.

The cross-linked PDMS-*b*-PS microporous film supported on glass substrate was pyrolyzed according to the procedures outlined in the Experimental section. XPS analysis indicates that the atomic concentration of carbon is around zero and the

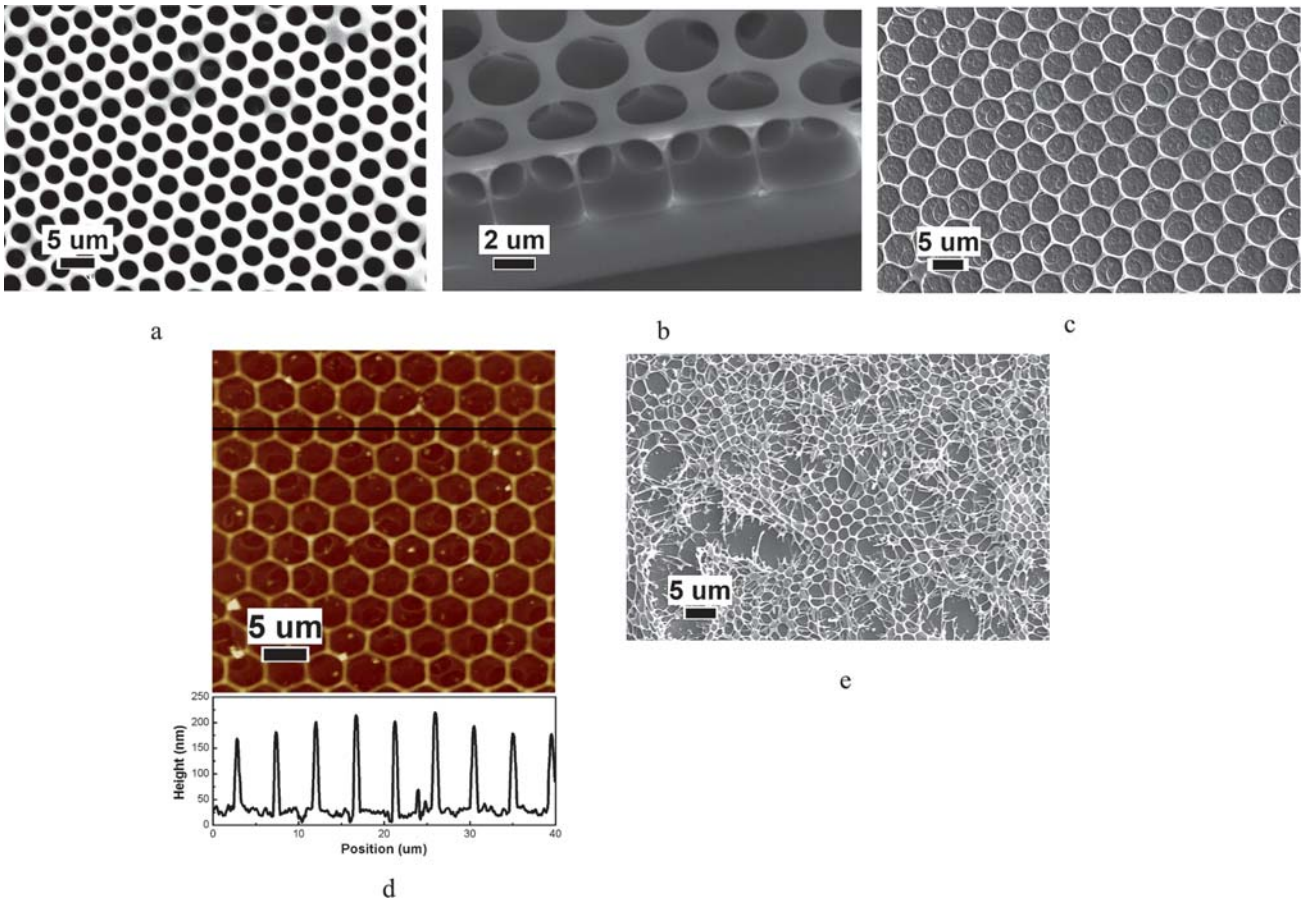

Fig. 3 SEM images of honeycomb structured PDMS-*b*-PS film after 4 h UV irradiation: (a) top view and (b) cross-sectional view; SEM (c) and topographic (d) images of the honeycomb structured silica patterns after pyrolysis; (e) random silica structures after pyrolyzing a multiple layer PDMS-*b*-PS microporous film.

silicon : oxygen ratio is close to 1 : 2 on the substrate (see ESI†, Fig. S2). This result then implies that the polymer matrix has been totally decomposed and PDMS has been successfully converted into silica. Although the microporous polymer film disappears, the rainbow color is still retained on the glass substrate (see ESI†, Fig. S3). Microscopy observation (Fig. 3c and d) reveals that the highly ordered silica patterns are created after the pyrolysis process. The walls of the obtained micropatterns become thinner and shaper, suggesting that more material is burned off. The ligaments that connect the inorganic picolitre holes are reduced from 1 μm to approximately 380 nm. However, the overall microscopic structures persist and are actually increased in sharpness. The silica micropatterns have identical spacing and size with that of the micropores on the as-prepared film surface. The silica patterns are tightly bound to the substrate, even after a long ultrasonic rinse with organic solvents.

The structure-directing action of the polymer matrix is ascribed to the prohibited unzipping and depropagation processes in cross-linked PS.[15] Linear PS is totally decomposed at 300 °C in air, whereas UV cross-linked PS had a char yield of 30% even at 450 °C for 1 h.[12e] The high char yield acts as the structure-directing agent in the subsequent pyrolysis process. Simultaneously, PDMS starts to convert into silica under 400 °C in air.[16] The skeleton of the microporous structures is gradually replaced by the formed silica during the pyrolysis, whilst the dense polymer stratum shrinks continuously and the microporous skeleton sinks down slowly. Eventually, ordered silica micropatterns are formed on substrate. A single layer of microporous structures is the key point for the formation of ordered ceramic micropatterns. For a multiple layer structured film, either cross-linking during the UV irradiation or the shrinkage during the pyrolyzing process is not uniform. Finally, only disordered silica structures are formed (Fig. 3e).

Microstructured ceramic containing Ti, Co or Fe

Microstructured ceramics have potential use in photonic crystals, while backfilling ceramic arrays with organic semiconductors would provide access to novel device architectures.[17] Fabrication of ceramic materials by shaping, cross-linking and thermolyzing a precursor polymer usually is related to a time-consuming and complicated synthesis. Directly scratching microstructures into thin ceramic films are also tedious. Generally, hybridization of organic polymer with inorganic structures may combine the merits of both components. The synthesis of organic/inorganic hybrid materials using organic polymers as structure directing agents or templates is an area of rapid growth.[6a,c,8] Based on the above discussion, the BF process offers a cost-effective and versatile technique to prepare micropatterns ceramic materials. Here, the preparation of microstructured TiO_2/SiO_2 ceramic is taken as an

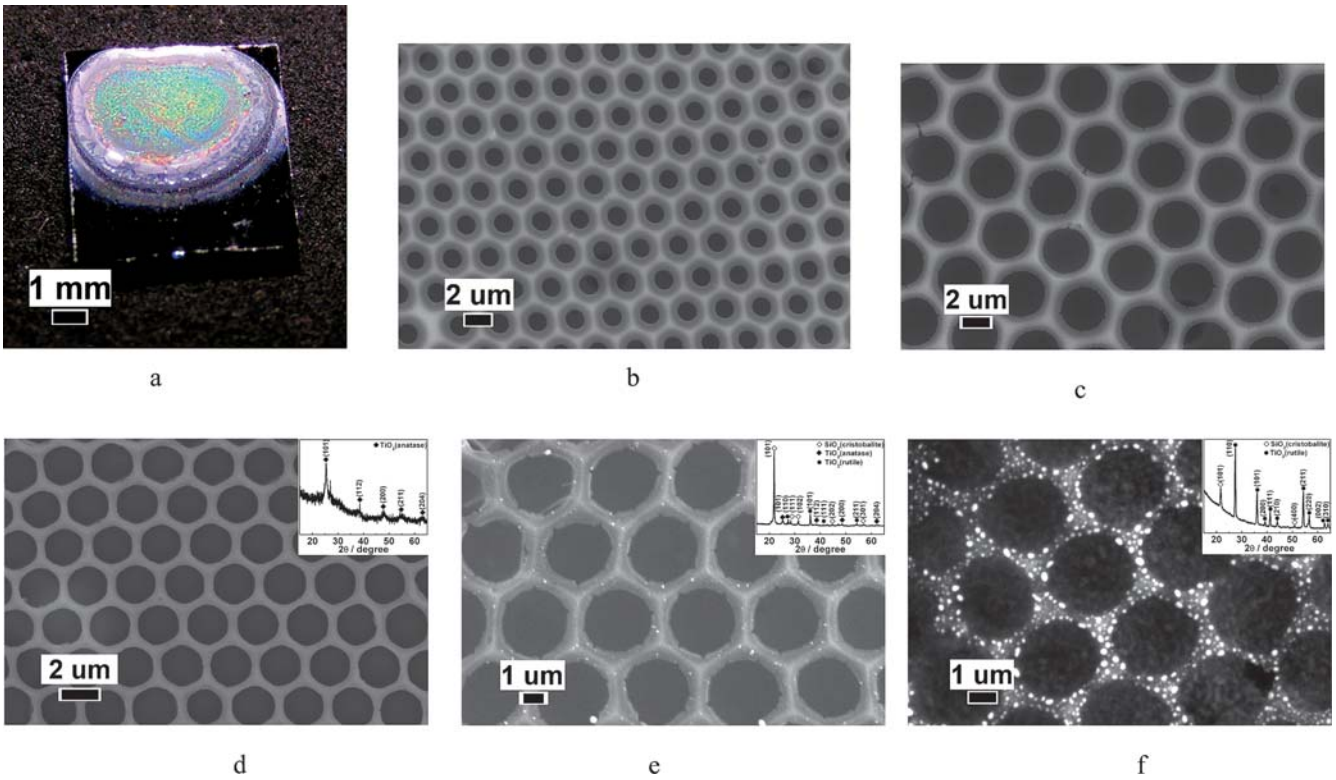

Fig. 4 (a) Photograph of sunlight diffraction obtained from a honeycomb structured PDMS-*b*-PS/Ti(OC_4H_9)$_4$ hybrid film on glass substrate casting from a solution of 40 mg mL^{-1}; Scanning electron micrographs of honeycomb structured hybrid film before (b) and after (c) 4 h UV irradiation; SEM images of the honeycomb structured ceramic patterns after pyrolysis at (d) 450 °C, (e) 700 °C and (f) 1000 °C. The X-ray results are shown in the insets.

example to illustrate how to obtain functionally active ceramic micropatterns. First, a mixture of PDMS-*b*-PS and Ti(OC_4H_9)$_4$ (3 : 1 w/w) was dissolved in CS_2 and cast on a silicon wafer by the same static BF process as mentioned above. The rainbow color (Fig. 4a) definitely demonstrates the formation of the ordered structured hybrid film on the Si wafer, though 25% weight ratio of functional precursor is incorporated into polymer matrix. No macro-phase separation is observed in the film, as confirmed by optical microscopy and SEM (Fig. 4b). After the same UV exposure, the honeycomb structures in the hybrid film are well preserved (Fig. 4c). In the subsequent pyrolysis process, regularly inorganic patterns with thinner walls are formed on substrates (Fig. 4d). The IR spectrum showed the total absence of any C–H stretching bands or organic functional-group bands, ascertaining that the hybrid film was converted into a microstructured ceramic.

GIXRD of the ceramic film indicates the formation of anatase phase after the pyrolysis process (inset in Fig. 4d). The TiO_2 (101) peak of the anatase-type structure is considered to be suitable for photocatalytic applications. The overall microscopic structures persist and are actually increased in sharpness further annealing to 700 °C (Fig. 4e). X-Ray results reveal the formation of SiO_2 and the phase transformation to rutile (inset in Fig. 4e). The pyrolysis in air has burned out the carbon, but at the same time has oxidized the silicon and the titanium, so that the oxidative removal of carbon is compensated for by the uptake of oxygen under formation of the ceramic oxide. A complete phase transformation to rutile occurs at 1000 °C (inset in Fig. 4f). Partial ceramic microstructures collapse because of the volume shrinkage during the phase transformation (Fig. 4f).

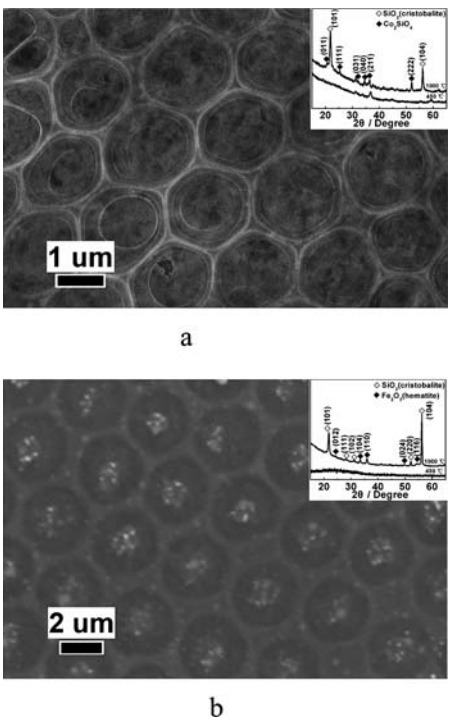

Fig. 5 (a) Si–Co–O ceramic microstructures after pyrolyzing a honeycomb structured PDMS-*b*-PS/Co(acac)$_3$ hybrid film at 1000 °C. (b) Si–Fe–O ceramic microstructures after pyrolyzing a honeycomb structured PDMS-*b*-PS/ferrocene hybrid film at 1000 °C. The X-ray results are shown in the insets.

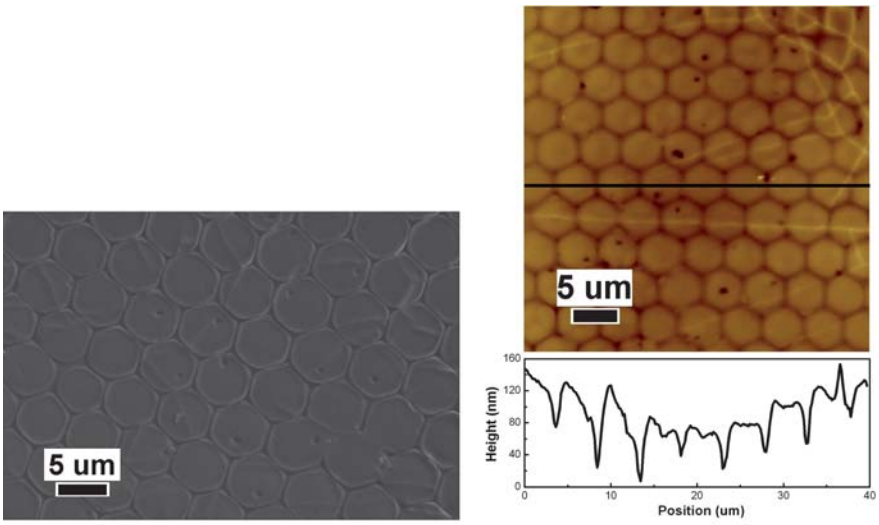

Fig. 6 SEM (a) and topographic (b) images of positive PDMS replica released from micropatterned substrate. The height profile of the PDMS replica was taken from the black line in the AFM image.

Similarly, the facile fabrication method is expanded to other systems, simply by changing different precursors. Si–Co–O (Fig. 5a) and Si–Fe–O (Fig. 5b) ceramic microstructures have been prepared by choosing $Co(acac)_3$ and ferrocene as the precursors after the same BF process, UV irradiation and pyrolysis. In the future, we plan to investigate the cobalt silicate ceramics for catalytic purposes and the ferrosilicate microstructures utilized as magnetic and electronic materials.[18] Additionally, some ternary systems are currently under investigation.

Replication of microstructured ceramic by PDMS stamp

The use of soft lithography or replica molding is a well-established technique reviewed by Xia and Whitesides.[19] A mold, mask or elastomeric stamp having relief structures on its surface is the key element of soft lithography. The time and expense involved in generating masks are significant barriers to the use of photolithography by chemists and biologists. These barriers have also limited the development of soft lithography, and inhibited the use of microfabrication in a number of areas. Besides the potential catalysis applications, the obtained micropatterned ceramic can serve as masters to replicate elastomeric stamps. Siloxane-based elastomers, in particular PDMS are a class of materials which have stable chemical inertness and low surface tension. Textured PDMS stamps have widespread use as transferring patterns for optical systems, microelectronic devices and sensors.[19c] Rapid prototyping allows the production of substantial numbers of simple microstructures rapidly and inexpensively.

A positive replica of the micropatterns was prepared by casting PDMS prepolymer (Sylgard184, Dow Corning Inc., USA) on the top of the substrate and removing the air trapped in the trenches under vacuum.[20] A 10 : 1 ratio (w/w) of the liquid precursor and curing agent were mixed and allowed to cure at room temperature on microstructured silica patterns. After crosslinking, the PDMS was peeled off from the template and SEM and AFM images were obtained (Fig. 6a and b). A hexagonal array of hemispherical textures on PDMS was seen, having the same diameter and depth as that of the micropatterns. The PDMS fully penetrated into the trenches and the micropatterns were replicated with high fidelity. The clefts shown in the microscopy images stem from the cracked Au coating on the PDMS stamp for SEM images, but not the defects on the silica template.

Conclusion

The static breath figure process is a robust method to fabricate highly ordered microporous polymer films and polymer/functional precursor hybrid films. Diblock copolymer PDMS-*b*-PS is employed to construct microporous polymer structures. The PS composition can be further cross-linked by UV irradiation without destroying the spatial morphology. The cross-linked polymer matrix acts as structure-directing agent in the subsequent pyrolysis process, whilst PDMS composition is converted into silica to form robust, honeycomb structured micropatterns on the substrate. Single layer microporous structures are crucial for the formation of regular patterns. The versatility of this fabrication process is demonstrated by preparing ordered ceramic micropatterns containing Ti, Co or Fe, simply through mixing different functional precursors. Moreover, the micropatterns on the substrate can be replicated by PDMS stamps. In the future, we plan to investigate these functionalized microstructured ceramics for catalytic, magnetic and electronic purposes and expand this facile fabrication method to other systems.

Acknowledgements

L. Li gratefully acknowledges the National Natural Science Foundation of China (No. 50703032 and 20974089) and the Program for New Century Excellent Talents of Ministry of Education of China (NCET-08-0475) and Natural Science Foundation of Fujian Province (2009J06029).

References

1 (*a*) E. Menard, M. A. Meitl, Y. G. Sun, J. U. Park, D. J. L. Shir, Y. S. Nam, S. Jeon and J. A. Rogers, *Chem. Rev.*, 2007, **107**, 1117; (*b*) M. Geissler and Y. N. Xia, *Adv. Mater.*, 2004, **16**, 1249; (*c*) A. S. Blawas and W. M. Reichert, *Biomaterials*, 1998, **19**, 595.

2 (*a*) M. Arbatti, X. B. Shan and Z. Y. Cheng, *Adv. Mater.*, 2007, **19**, 1369; (*b*) H. Matsubara, S. Yoshimoto, H. Saito, J. L. Yue, Y. Tanaka and S. Noda, *Science*, 2008, **319**, 445; (*c*) J. Garcia-Barriocanal, A. Rivera-Calzada, M. Varela, Z. Sefrioui, E. Iborra, C. Leon, S. J. Pennycook and J. Santamaria, *Science*, 2008, **321**, 676; (*d*) E. Formo, M. S. Yavuz, E. P. Lee, L. Lane and Y. N. Xia, *J. Mater. Chem.*, 2009, **19**, 3878.

3 (*a*) D. W. Xu, E. Graugnard, J. S. King, L. W. Zhong and C. J. Summers, *Nano Lett.*, 2004, **4**, 2223; (*b*) S. B. Clendenning, S. Aouba, M. S. Rayat, D. Grozea, J. B. Sorge, P. M. Brodersen, R. N. S. Sodhi, Z. H. Lu, C. M. Yip, M. R. Freeman, H. E. Ruda and I. Manners, *Adv. Mater.*, 2004, **16**, 215; (*c*) C. X. Xiang, Y. G. Yang and R. M. Penner, *Chem. Commun.*, 2009, 859; (*d*) O. D. Velev and E. W. Kaler, *Adv. Mater.*, 2000, **12**, 531; (*e*) L. Yang, Y. Y. Lua, M. V. Lee and M. R. Linford, *Acc. Chem. Res.*, 2005, **38**, 933.

4 (*a*) M. Park, C. Harrison, P. M. Chaikin, R. A. Register and D. H. Adamson, *Science*, 1997, **276**, 1401; (*b*) Y. Li, T. Sasaki, Y. Shimizu and N. Koshizaki, *Small*, 2008, **4**, 2286; (*c*) X. Chen, Z. M. Chen, N. Fu, G. Lu and B. Yang, *Adv. Mater.*, 2003, **15**, 1413.

5 (*a*) G. Widawski, M. Rawiso and B. Francois, *Nature*, 1994, **369**, 387; (*b*) U. H. F. Bunz, *Adv. Mater.*, 2006, **18**, 973; (*c*) M. H. Stenzel, C. Barner-Kowollik and T. P. Davis, *J. Polym. Sci., Part A: Polym. Chem.*, 2006, **44**, 2363.

6 (*a*) B. C. Englert, S. Scholz, P. J. Leech, M. Srinivasarao and U. H. F. Bunz, *Chem.–Eur. J.*, 2005, **11**, 995; (*b*) L. A. Connal and G. G. Qiao, *Adv. Mater.*, 2006, **18**, 3024; (*c*) O. Karthaus, X. Cieren, N. Maruyama and M. Shimomura, *Mater. Sci. Eng. C: Biomimetic Supramol. Syst.*, 1999, **10**, 103; (*d*) Y. Tian, S. Liu, H. Ding, L. Wang, B. Liu and Y. Shi, *Polymer*, 2007, **48**, 2338; (*e*) T. Hayakawa and S. Horiuchi, *Angew. Chem., Int. Ed.*, 2003, **42**, 2285.

7 (*a*) H. Yabu and M. Shimomura, *Langmuir*, 2005, **21**, 1709; (*b*) B. de Boer, U. Stalmach, H. Nijland and G. Hadziioannou, *Adv. Mater.*, 2000, **12**, 1581; (*c*) H. Takamori, T. Fujigaya, Y. Yamaguchi and N. Nakashima, *Adv. Mater.*, 2007, **19**, 2535.

8 K. Zhang, L. W. Zhang and Y. M. Chen, *Macromol. Rapid Commun.*, 2007, **28**, 2024.

9 (*a*) M. Srinivasarao, D. Collings, A. Philips and S. Patel, *Science*, 2001, **292**, 79; (*b*) J. Peng, Y. C. Han, Y. M. Yang and B. Y. Li, *Polymer*, 2004, **45**, 447; (*c*) L. L. Song, R. K. Bly, J. N. Wilson, S. Bakbak, J. O. Park, M. Srinivasarao and U. H. F. Bunz, *Adv. Mater.*, 2004, **16**, 115.

10 L. Ghannam, M. Manguian, J. Francois and L. Billon, *Soft Matter*, 2007, **3**, 1492.

11 D. Beysens, A. Steyer, P. Guenoun, D. Fritter and C. M. Knobler, *Phase Transitions*, 1991, **31**, 219.

12 (*a*) H. Yabu, M. Kojima, M. Tsubouchi, S. Onoue, M. Sugitani and M. Shimomura, *Colloids Surf., A*, 2006, **284–285**, 254; (*b*) B. Erdogan, L. L. Song, J. N. Wilson, J. O. Park, M. Srinivasarao and U. H. F. Bunz, *J. Am. Chem. Soc.*, 2004, **126**, 3678; (*c*) O. Karthaus, Y. Hashimoto, K. Kon and Y. Tsuriga, *Macromol. Rapid Commun.*, 2007, **28**, 962; (*d*) L. Li, C. K. Chen, A. J. Zhang, X. Y. Liu, K. Cui, J. Huang, Z. Ma and Z. H. Han, *J. Colloid Interface Sci.*, 2009, **331**, 446; (*e*) L. Li, Y. W. Zhong, J. Li, C. K. Chen, A. J. Zhang, J. Xu and Z. Ma, *J. Mater. Chem.*, 2009, **19**, 7222.

13 L. Li, Y. W. Zhong, C. Y. Ma, J. Li, C. K. Chen, A. J. Zhang, D. L. Tang, S. Y. Xie and Z. Ma, *Chem. Mater.*, 2009, **21**, 4977.

14 (*a*) B. Rånby and J. F. Rabek, *Photodegradation, Photooxidation and Photostabilization of Polymers*, Wiley, New York, 1975; (*b*) M. J. Melo, S. Bracci, M. Camaiti, O. Chiantore and F. Piacenti, *Polym. Degrad. Stab.*, 1999, **66**, 23.

15 G. F. Levchik, K. Si, S. V. Levchik, G. Camino and C. A. Wilkie, *Polym. Degrad. Stab.*, 1999, **65**, 395.

16 G. Camino, S. M. Lomakin and M. Lazzari, *Polymer*, 2001, **42**, 2395.

17 (*a*) L. Feng, S. H. Li, Y. S. Li, H. J. Li, L. J. Zhang, J. Zhai, Y. L. Song, B. Q. Liu, L. Jiang and D. B. Zhu, *Adv. Mater.*, 2002, **14**, 1857; (*b*) L. Feng, Y. L. Song, J. Zhai, B. Q. Liu, J. Xu, L. Jiang and D. B. Zhu, *Angew. Chem., Int. Ed.*, 2003, **42**, 800; (*c*) J. Y. Shiu, C. W. Kuo, P. L. Chen and C. Y. Mou, *Chem. Mater.*, 2004, **16**, 561; (*d*) A. Lafuma and D. Quere, *Nat. Mater.*, 2003, **2**, 457.

18 (*a*) E. van Steen, G. S. Sewell, R. A. Makhothe, C. Micklethwaite, H. Manstein, M. de Lange and C. T. O'Connor, *J. Catal.*, 1996, **162**, 220; (*b*) B. Ernst, S. Libs, P. Chaumette and A. Kiennemann, *Appl. Catal., A*, 1999, **186**, 145; (*c*) K. Kulbaba, R. Resendes, A. Cheng, A. Bartole, A. Safa-Sefat, N. Coombs, H. D. H. Stover, J. E. Greedan, G. A. Ozin and I. Manners, *Adv. Mater.*, 2001, **13**, 732; (*d*) S. B. Clendenning, S. Fournier-Bidoz, A. Pietrangelo, G. C. Yang, S. J. Han, P. M. Brodersen, C. M. Yip, Z. H. Lu, G. A. Ozin and I. Manners, *J. Mater. Chem.*, 2004, **14**, 1686.

19 (*a*) J. L. Wilbur, A. Kumar, E. Kim and G. M. Whitesides, *Adv. Mater.*, 1994, **6**, 600; (*b*) Y. N. Xia and G. M. Whitesides, *Langmuir*, 1997, **13**, 2059; (*c*) Y. N. Xia and G. M. Whitesides, *Angew. Chem., Int. Ed.*, 1998, **37**, 550.

20 D. H. Kim, Z. Q. Lin, H. C. Kim, U. Jeong and T. P. Russell, *Adv. Mater.*, 2003, **15**, 811.